Springer

KSME

Journal of Mechanical Science and Technology 25 (7) (2011) 1837~1844
www.springerlink.com/content/1738-494x
DOI 10.1007/s12206-011-0423-y

# Hydrodynamic plane and axisymmetric slip stagnation-point flow with thermal radiation and temperature jump †

Jing Zhu[1,*], Liancun Zheng[1] and Xinxin Zhang[2]

[1]*Department of Mathematics and Mechanics, University of Science and Technology Beijing, Beijing , 100083, China*
[2]*Thermal Engineering Department, University of Science and Technology Beijing, Beijing, 100083, China*

(Manuscript Received January 27, 2010; Revised March 6, 2011; Accepted April 10, 2011)

**Abstract**

This work focuses on the steady boundary layer flow and heat transfer near the forward stagnation point of plane and axisymmetric sheet towards a stretching sheet with velocity slip and temperature jump. The resulting nonlinear partial differential equations are reduced to the system of nonlinear ordinary differential equations by means of similarity transformations. The analytical solutions for the velocity and temperature distributions are obtained for the various values of the ratio of free stream velocity and stretching velocity, velocity slip parameter, magnetic parameter, the suction parameter, temperature jump parameter, Prandtl number, the radiation parameter and dimensionality index parameter in the series forms with the help of homotopy analysis method. Convergence of the series is explicitly discussed. The flow and shear stresses depend heavily on the velocity slip parameter. The temperature gradient at the wall increases with velocity slip parameter, temperature jump factor and decreased thermal radiation.

*Keywords*: Slip flow; Stagnation point; Thermal radiation; Homotopy analysis method; Temperature jump

## 1. Introduction

Stagnation flow, which describes the fluid motion near the stagnation region, exists on all solid bodies moving in a fluid. There has been considerable interest in investigating plane and axisymmetric flow near a stagnation point on a surface. Hiemenz [1] was the first to discover that the stagnation point flow can be analyzed exactly by the Navier-Stokes equations, and he reported two-dimensional plane flow velocity distribution. Later, Chiam [2] investigated two dimensional normal and oblique stagnation-point flows of an incompressible viscous fluid towards a stretching surface while Mahapatra and Gupta [3] studied the heat transfer of normal stagnation flow to a stretching sheet. Recently Anuar Ishak et al. [4] investigated mixed convection flow near a stagnation point on a vertical surface.

On the other hand, the radiative effects have important applications in physics and engineering, particularly in space technology and high temperature processes. Raptis [5] had considered thermal radiation effects on the flow of micropolar fluids past a continuously moving plate. El-Arabawy [6] studied the effect of suction or injection on the flow of a micropolar fluid past a continuously moving plate with radiation. Recently, Khan [7] studied heat transfer in a viscoelastic fluid flow over a stretching surface with heat source and radiation.

In all the above mentioned studies, no attention has been given to the effects of partial slip on the flow. The no-slip boundary condition is known as the central tenet of the Navier–Stokes theory. However, there are situations wherein this condition is not appropriate. Partial velocity slip may occur on the stretching boundary when the fluid is particulate such as emulsions, suspensions, foams and polymer solutions [8]. The effects of slip conditions are very important for some fluids which exhibit wall slip. Fluids exhibiting slip are important in technological applications, such as in the polishing of artificial heart valves and internal cavities. Therefore, a better understanding of the phenomenon of slip is necessary. Mooney [9] initiated the study of boundary layer flow with partial slip; many researchers [10-11] had confirmed the phenomenon of wall slip fluid. Hayat et al. [12] examined the effect of the slip boundary condition on the flow of fluids in a channel. The non-Newtonian flows with wall slip have been studied numerically in Refs. [13-15].

The stagnation slip flow on a fixed plate and on a moving one was considered numerically by Wang [16-17]. It was found that slip greatly affects the flow field. The present paper extends the results of previous authors by considering the effect of velocity slip and temperature jump. The method we

† This paper was recommended for publication in revised form by Associate Editor Jun Sang Park

*Corresponding author. Tel.: +86 010 62332891, Fax.: +86 010 62332891
E-mail address: hahazhujing@sohu.com

© KSME & Springer 2011

employed here is based on the homotopy analytical method (HAM [18]) of solving non-linear equations, which has already been applied to some other problems [19-21].

## 2. Mathematical formulation

### 2.1 Flow analysis

Consider the steady flow of a laminar, viscous and incompressible, electrically conducting fluid near the stagnation point of a flat sheet coinciding with the plane $y = 0$, and the flow being confined to $y > 0$. $x$ and $y$ are the Cartesian coordinates with the origin at the stagnation point along and normal to the plate, respectively. A uniform magnetic field is applied in the $y$-direction causing a flow resistive force in the $x$-direction. The magnetic Reynolds number is assumed to be small, so that the induced magnetic field will be neglected. Under these conditions and taking into account the boundary layer approximation, the system of continuity, momentum can be written as:

$$\frac{\partial}{\partial x}\left(x^k u\right)+\frac{\partial}{\partial y}\left(x^k v\right)=0, \tag{1}$$

$$u\frac{\partial u}{\partial x}+v\frac{\partial u}{\partial y}=-\frac{1}{\rho}\frac{\partial P}{\partial x}+\nu\left(\frac{\partial^2 u}{\partial x^2}+\frac{\partial}{\partial x}\left(\frac{u^k}{x^k}\right)+\frac{\partial^2 u}{\partial y^2}\right)+\frac{\sigma B_0^2}{\rho}(u_e-u), \tag{2}$$

$$u\frac{\partial v}{\partial x}+v\frac{\partial v}{\partial y}=-\frac{1}{\rho}\frac{\partial P}{\partial y}+\nu\left(\frac{\partial^2 v}{\partial x^2}+\frac{k}{x}\frac{\partial v}{\partial x}+\frac{\partial^2 v}{\partial y^2}\right), \tag{3}$$

subject to boundary conditions

$$u(x,0)=cx+\frac{2-\sigma_v}{\sigma_v}\lambda_0\left.\frac{\partial u}{\partial y}\right|_{y=0}, \tag{4}$$

$$v(x,0)=-v_w,\ u(x,\infty)=u_e=ax. \tag{5}$$

$k$ is the index with $k$=1, Eqs. (1)-(5) are axially symmetric stagnation-point flows, while with $k$=0 is the plane flow. The $x$-axis is the tangential direction and $x$ is interpreted as the radial direction for axisymmetric flow situations. $u$ and $v$ are the velocity components along the $x$-axes and $y$-axes, respectively. $\rho$ is the density, $\nu$ is the kinematic viscosity, $\sigma$ is the fluid electrical conductivity, $B_0$ is the magnetic induction. $\lambda_0$ is the mean free path and $\sigma_v$ is the tangential momentum accommodation coefficient. The constant $c\ (>0)$ is proportional to the free stream velocity far away from the surface. $u_e = ax$ is free stream velocity of family shapes, in which $a$ is a positive constant

The velocity components are

$$u=\frac{x}{k+1}F'(y),\ v=-F(y). \tag{6}$$

Further, the following dimensionless quantities and transformations are introduced:

$$f(\eta)=\frac{F(y)}{((k+1)c\nu)^{\frac{1}{2}}},\quad \eta=y\left(\frac{(k+1)c}{\nu}\right)^{\frac{1}{2}}. \tag{7}$$

Inserting Eqs. (6) and (7) into Eqs. (1)-(3), results in

$$f'''+ff''-n(f')^2+nd^2-nM(f'-d)=0. \tag{8}$$

The boundary conditions in Eqs. (4) and (5) may be expressed in dimensionless form as

$$f(0)=R,\ f'(0)=1+\lambda f''(0),\ \ f'(\infty)=d, \tag{9}$$

where the local Knudsen number $Kn_x$ ($0.01 < Kn_x < 0.1$), the local Reynolds number $\mathrm{Re}_x$, velocity slip parameter $\lambda$, the Hartmann number $M$, the suction/injection velocity parameter $R$, velocity ratio parameter $d$ and the dimensionality index $n$ are defined, respectively, as:

$$Kn_x=\frac{\lambda_0}{\sqrt{d}\,x},\ \ \mathrm{Re}_x=\frac{u_e x}{\nu},\ \ \lambda=\frac{2-\sigma_v}{\sigma_v}Kn_x\,\mathrm{Re}_x^{\frac{1}{2}},$$

$$n=\frac{1}{1+k}\quad M=\frac{\sigma B_0^2}{c\rho},\ \ R=\frac{v_w}{\sqrt{a\nu}},\quad d=\frac{a}{c}.$$

### 2.2 Heat transfer analysis

By using usual boundary layer approximations, the equation of the energy for temperature $T$ in the presence of radiation may be written as

$$\rho c_p\left(u\frac{\partial T}{\partial x}+v\frac{\partial T}{\partial y}\right)=\kappa\left(\frac{1}{x^k}\frac{\partial}{\partial x}\left(x^k\frac{\partial T}{\partial x}\right)+\frac{\partial^2 T}{\partial y^2}\right)-\frac{\partial q_r}{\partial y}. \tag{10}$$

The appropriate boundary conditions are temperature jump at the wall

$$T(x,0)=T_w+S_0\left.\frac{\partial T}{\partial y}\right|_{y=0},\quad T(x,\infty)=T_\infty \tag{11}$$

where $T_w$ is the wall temperature, $T_\infty$ is the temperature of the fluid far from the sheet, $c_p$ is the specific heat capacity, $\kappa$ is the thermal conductivity , $q_r$ is the radiative heat flux and $S_0$ is the temperature jump coefficient.

Using the Rosseland approximation for radiation [22] for an optically thick layer, one can obtain

$$q_r=-\frac{4\sigma^*}{3k^*}\frac{\partial T^4}{\partial y} \tag{12}$$

where $\sigma^*$ and $k^*$ are the Stefan-Boltzmann constant and the mean absorption coefficient, respectively. We assume that the temperature differences within the flow such as that the term $T^4$ may be expressed as a linear function of temperature. Hence, expanding $T^4$ in a Taylor series about $T_\infty$ and neglecting higher-order terms we get

$$T^4 \cong 4T_\infty^3 T - T_\infty^4 . \tag{13}$$

In view of Eqs. (12) and (13), Eq. (10) reduces to

$$u\frac{\partial T}{\partial x} + v\frac{\partial T}{\partial y} = \left(\frac{\kappa}{\rho c_p} + \frac{16\sigma^* T_\infty^3}{3k^* \rho c_p}\right)\frac{\partial^2 T}{\partial y^2} . \tag{14}$$

From the above equation, it can be seen that the effect of radiation is to enhance the thermal diffusivity. Introducing the following dimensionless quantities

$$\theta = \frac{T - T_\infty}{T_w - T_\infty} . \tag{15}$$

When Eq. (15) is inserted in Eq. (14), we obtain

$$\theta'' + \Pr K_0 f \theta' = 0 \tag{16}$$

which is to be solved subject to

$$\theta(0) = 1 + \beta\theta'(0) , \qquad \theta(\infty) = 0 . \tag{17}$$

In the above equation, the thermal diffusivity $\alpha$ , the Prandtl number Pr, temperature jump factor $\beta$ and the radiation parameter $K_0$ are defined, respectively, as:

$$\alpha = \frac{\kappa}{\rho c_p} , \Pr = \frac{\nu}{\alpha} , \beta = \frac{S_0 \rho}{\sqrt{a/\nu}} , R_d = \frac{k^* \kappa}{4\sigma^* T_\infty^3} , \quad K_0 = \frac{3R_d}{3R_d + 4} .$$

## 3. HAM solution for $f(\eta)$ and $\theta(\eta)$

### *3.1 Zeroth-order deformation equations*

Under the first rule of solution expression, the initial guess approximations for the HAM solution are

$$f_0(\eta) = R + d\eta + \frac{(1-d)\eta e^{-\eta}}{1+2\lambda} , \quad \theta_0(\eta) = \eta e^{-\eta} + e^{-\eta}$$

and the auxiliary linear operators are

$$L_f(f) = f''' + f'' , L_\theta(\theta) = \theta'' - \theta' .$$

The operators above equation satisfy

$$L_f[C_1 + C_2\eta + C_3 e^{-\eta}] = 0 , L_\theta[C_4 + C_5 e^{-\eta}] = 0$$

in which $C_i, i = 1,2,3,4,5$ are arbitrary constants.

The zeroth order deformation problems are

$$(1-q)L_f[F(\eta;q) - f_0(\eta)] = qh_f N_f[F(\eta;q)] , \tag{18}$$
$$(1-q)L_\theta[\Theta(\eta;q) - \theta_0(\eta)] = qh_\theta N_\theta[\Theta(\eta;q)] , \tag{19}$$
$$F(0,q) = R , F'(0,q) = 1 + \lambda F''(0,q) , F'(\infty,q) = d , \tag{20}$$
$$\Theta(0,q) = 1 + \beta\Theta'(0,q) , \quad \Theta(\infty,q) = 0 . \tag{21}$$

where $N_f[F(\eta;\, q)]$ and $N_\theta[\Theta(\eta;\, q)]$ are

$$N_f[F(\eta;q)] = \frac{\partial^3 F}{\partial \eta^3} + F\frac{\partial^2 F}{\partial \eta^2} - n\left(\frac{\partial F}{\partial \eta}\right)^2 + nd^2 - nM\left(\frac{\partial F}{\partial \eta} - d\right),$$
$$N_\theta[\Theta(\eta;q)] = \frac{\partial^2 \Theta}{\partial \eta^2} + \Pr K_0 F\frac{\partial\, \Theta}{\partial \eta} .$$

In the above equations, $q \in [0, 1]$ is the embedding parameter, $h_f$ and $h_\theta$ are auxiliary non-zero parameters. Due to Taylor's theorem, one can write

$$F = f_0(\eta) + \sum_{m=1}^{+\infty} f_m(\eta) q^m , f_m(\eta) = \frac{1}{m!}\frac{\partial^m F(\eta;q)}{\partial \eta^m}\bigg|_{q=0} ; \tag{22}$$

$$\Theta = \theta_0(\eta) + \sum_{k=1}^{+\infty} \theta_m(\eta) q^m , \theta_m(\eta) = \frac{1}{m!}\frac{\partial^m \Theta(\eta;q)}{\partial \eta^m}\bigg|_{q=0} . \tag{23}$$

### *3.2 High-order deformation equations*

Differentiating the zeroth-order deformation in Eqs. (18)-(21) *k* times with respect to *q*, then dividing by *k*! and finally setting *q* =0, we get the following *kth*-order deformation equations:

$$L_f\left[f_k(\eta) - \chi_k f_{k-1}(\eta)\right] = \hbar_f R_{fk}\left(\vec{f}_{k-1}\right) , \tag{24}$$

$$L_\theta\left[\theta_k(\eta) - \chi_k \theta_{k-1}(\eta)\right] = \hbar_\theta R_{\theta k}\left(\vec{\theta}_{k-1}\right) , \tag{25}$$

$$f_k(0) = f_k'(\infty) = 0, f_k'(0) = \lambda f_k''(0) , \tag{26}$$

$$\theta_k(0) = \beta\theta_k'(0), \quad \theta_k(\infty) = 0 \tag{27}$$

where

$$R_{\theta k}\left(\vec{\theta}_{k-1}\right) = \theta_{k-1}''(\eta) + \Pr K_0 \sum_{s=0}^{k-1} f_s(\eta)\theta_{k-1-s}'(\eta) ,$$
$$R_{fk}\left(\vec{f}_{k-1}\right) = \sum_{s=0}^{k-1}\left(f_s(\eta) f_{k-1-s}''(\eta) - nf_s'(\eta) f_{k-1-s}'(\eta)\right) + f_{k-1}'''(\eta) - nMf_{k-1}'(\eta) + n(1-\chi_k)(d^2 + dM),$$

and

$$\chi_k = \begin{cases} 0 & k = 1 \\ 1 & k > 1 \end{cases} .$$

If auxiliary non-zero parameters $\hbar_f$ and $\hbar_\theta$ are properly chosen, the homotopy-series solutions of Eqs. (22) and (23) may converge quickly. In theory, one can define the exact square residual error for the $k$th-order of approximation.

$$\Delta_k(f)=\int_0^{+\infty}\left(\left[N_f\sum_{i=0}^{k}f_i(x)\right]\right)^2 dx\,,$$
$$\Delta_k(\theta)=\int_0^{+\infty}\left(\left[N_\theta\sum_{j=0}^{k}\theta_j(x)\right]\right)^2 dx\,.$$

### 3.3 Recursive formulae

We have the solution of problem as

$$f_m(\eta)=\sum_{k=0}^{m+1}\sum_{i=0}^{2m+2-k}a_{m,k}^i\eta^i\exp(-k\eta)\,, \tag{28}$$
$$\theta_m(\eta)=\sum_{k=1}^{m+1}\sum_{i=0}^{2m+2-k}b_{m,k}^i\eta^i\exp(-k\eta)\,. \tag{29}$$

Substituting Eqs. (28) and (29) into Eqs. (24)-(27), the recurrence formulae for the coefficients $a_{m,k}^i$ of $f_m(\eta)$ and $b_{m,k}^i$ of $\theta_m(\eta)$ are obtained for $m\ge 1$:

$$\begin{aligned}
a_{m,0}^0 &= \chi_m a_{m-1,0}^0+\sum_{k=2}^{m+1}\sum_{q=0}^{2m+2-k}(k+k^2\lambda-1)\mu_{k,0}^q\Omega_{m,k}^q\\
&-\sum_{q=0}^{2m}(\lambda+1)\mu_{1,1}^q\Omega_{m,1}^q+\sum_{k=2}^{m+1}\sum_{q=2}^{2m+2-k}\mu_{k,2}^q\Omega_{m,k}^q\\
&-\sum_{k=2}^{m+1}\sum_{q=1}^{2m+2-k}(1+2k\lambda)\mu_{k,1}^q\Omega_{m,k}^q-\sum_{q=1}^{2m}2\lambda\mu_{1,2}^q\Omega_{m,1}^q,
\end{aligned}$$

$$b_{m,0}^0=\chi_m b_{m-1,0}^0=0\ ,\quad a_{m,0}^i=b_{m,0}^i=0\ ,\ 1\le i\le 2m+2;$$

$$b_{m,0}^i=\chi_m b_{m-1,0}^i=0\ \ ,1\le i\le 2m,\quad b_{m,0}^i=0\ \ ,2m+1\le i\le 2m+2;\ ,$$

$$\begin{aligned}
a_{m,1}^0 &= \chi_m a_{m-1,1}^0-\sum_{k=2}^{m+1}\sum_{q=0}^{2m+2-k}(k+\lambda k^2)\mu_{k,0}^q\Omega_{m,k}^q\\
&+\sum_{k=2}^{m+1}\sum_{q=1}^{2m+2-k}(1+2k\lambda)\mu_{k,1}^q\Omega_{m,k}^q+\sum_{q=0}^{2m}(1+\lambda)\mu_{1,1}^q\Omega_{m,1}^q\\
&-\sum_{k=2}^{m+1}\sum_{q=2}^{2m+2-k}2\lambda\mu_{k,0}^q\Omega_{m,k}^q+\sum_{q=1}^{2m}2\lambda\mu_{1,2}^q\Omega_{m,1}^q,
\end{aligned}$$

$$\begin{aligned}
b_{m,1}^0 &= \chi_m b_{m-1,1}^0+\sum_{k=2}^{m+1}\sum_{q=1}^{2m+2-k}\frac{\beta}{1+\beta}\Lambda_{k,1}^q\Upsilon_{m,k}^q\\
&+\sum_{k=2}^{m+1}\sum_{q=0}^{2m+2-k}\frac{1-k\beta}{1+\beta}\Lambda_{k,0}^q\Upsilon_{m,k}^q-\sum_{q=0}^{2m}\frac{1}{1+\beta}\Lambda_{1,1}^q\Upsilon_{m,1}^q,
\end{aligned}$$

$$a_{m,1}^i=\chi_m a_{m-1,1}^i+\sum_{q=i-1}^{2m}\mu_{1,i}^q\Omega_{m,1}^q,\quad 1\le i\le 2m-1\,,$$

$$b_{m,1}^i=\chi_m b_{m-1,1}^i+\sum_{q=i-1}^{2m}\Lambda_{1,i}^q\Upsilon_{m,1}^q,\quad 1\le i\le 2m-1\,,$$

$$a_{m,1}^i=\sum_{q=i-1}^{2m}\mu_{1,i}^q\Omega_{m,1}^q,\quad b_{m,1}^i=\sum_{q=i-1}^{2m}\Lambda_{1,i}^q\Upsilon_{m,1}^q,\ 2m\le i\le 2m+1\,,$$

$$a_{m,k}^0=\chi_m a_{m-1,k}^0+\sum_{q=0}^{2m+2-k}\mu_{k,i}^q\Omega_{m,k}^q,\quad 2\le k\le m\,,$$

$$b_{m,k}^0=\chi_m b_{m-1,k}^0+\sum_{q=0}^{2m+2-k}\Lambda_{k,i}^q\Upsilon_{m,k}^q,\quad 2\le k\le m\,,$$

$$a_{m,k}^i=\chi_m a_{m-1,k}^i+\sum_{q=i}^{2m+2-k}\mu_{k,i}^q\Omega_{m,k}^q,\quad 2\le k\le m,\ 1\le i\le 2m-k,$$

$$b_{m,k}^i=\chi_m b_{m-1,k}^i+\sum_{q=i}^{2m+2-k}\Lambda_{k,i}^q\Upsilon_{m,k}^q,\quad 2\le k\le m,\ 1\le i\le 2m-k,$$

$$a_{m,k}^i=\sum_{q=i}^{2m+2-k}\mu_{k,i}^q\Omega_{m,k}^q,\quad 2\le k\le m,\ 2m+1-k\le i\le 2m+2-k,$$

$$b_{m,k}^i=\sum_{q=i}^{2m+2-k}\Lambda_{k,i}^q\Upsilon_{m,k}^q,\quad 2\le k\le m,\ 2m+1-k\le i\le 2m+2-k,$$

$$a_{m,m+1}^i=\sum_{q=i}^{m+1}\mu_{m+1,i}^q\Omega_{m,m+1}^q\ ,\ b_{m,m+1}^i=\sum_{q=i}^{m+1}\Lambda_{m+1,i}^q\Upsilon_{m,m+1}^q\ ,$$

where

$$\mu_{k,i}^u=\frac{i!(u-i+2)}{u!},\quad k=1,0\le i\le u+1,$$

$$\mu_{k,i}^u=\frac{u!}{i!(k-1)^{u-i+1}}\{1-(\frac{1}{n})^{u-i+1}[(u-i+2)-(u-i+1)(\frac{1}{n})]\},$$
$$(k\ge 2,0\le i\le u)$$

$$\Lambda_{k,i}^q=\frac{q!}{i!},\quad k=1,\quad 0\le i\le q+1,$$

$$\Lambda_{k,i}^q=\frac{q!}{i!(k-1)^{q-i+1}}\{1-(\frac{1}{n})^{q-i+1}\},k\ge 2,0\le i\le q.$$

$$\Omega_{m,1}^i=h_f(e_{m-1,1}^i-nMc_{m-1,1}^i)+(\delta_{m,1}^i+n\Delta_{m,1}^i),\quad 0\le i\le 2m-1\,,$$

$$\Omega_{m,1}^{2m}=\delta_{m,1}^{2m}+n\Delta_{m,1}^{2m},\quad \Omega_{m,m+1}^i=\delta_{m,m+1}^i+n\Delta_{m,m+1}^i,\ 0\le i\le m+1\,,$$

$$\Omega_{m,k}^i=h_f(e_{m-1,1}^i-nMc_{m-1,1}^i)+\delta_{m,k}^i+n\Delta_{m,k}^i,\ 0\le i\le 2m-k,2\le k\le m,$$

$$\Omega_{m,k}^i=\delta_{m,k}^i+n\Delta_{m,k}^i,\quad 2m+1-k\le i\le 2m+2-k,\quad 2\le k\le m.$$

$$\Upsilon_{m,1}^i=h_\theta t_{m-1,1}^i+\Pr K_0\Xi_{m,1}^i,\quad 0\le i\le 2m-1,$$

$$\Upsilon_{m,1}^{2m}=\Pr K_0\Xi_{m,1}^{2m},\quad \Upsilon_{m,m+1}^i=\Pr K_0\Xi_{m,m+1}^i,\ 0\le i\le m+1\,,$$

$$\Upsilon_{m,k}^i=h_\theta t_{m-1,k}^i+\Pr K_0\Xi_{m,k}^i,(0\le i\le 2m-k,2\le k\le m)\ ,$$

$$\Upsilon_{m,k}^i=\Pr K_0\Xi_{m,k}^i,\ 2m+1-k\le i\le 2m+2-k,2\le k\le m\ .$$

The coefficients $\delta_{m,k}^i$, $\Delta_{m,k}^i$ and $\Xi_{m,k}^i$ for $m\ge 1$ are

$$\delta_{m,k}^i=\sum_{s=0}^{m-1}\sum_{r=\max\{1,k+s-m\}}^{\min\{s+1,k-1\}}\sum_{t=\max\{0,i+2s+k-r-2m\}}^{\min\{2s+2-r,i\}}a_{m-1-s,k-r}^{i-t}d_{s,r}^t,$$

$$\Delta_{m,k}^i=\sum_{s=0}^{m-1}\sum_{r=\max\{1,k+s-m\}}^{\min\{s+1,k-1\}}\sum_{t=\max\{0,i+2s+k-r-2m\}}^{\min\{2s+2-r,i\}}c_{m-1-s,k-r}^{i-t}c_{s,r}^t,$$

$$\Xi_{m,k}^i=\sum_{s=0}^{m-1}\sum_{r=\max\{1,k+s-m\}}^{\min\{s+1,k-1\}}\sum_{t=\max\{0,i+2s+k-r-2m\}}^{\min\{2s+2-r,i\}}a_{m-1-s,k-r}^{i-t}s_{s,r}^t,$$

and the coefficients $c_{m,k}^i$, $e_{m,k}^i$ $s_{m,k}^i$, $d_{m,k}^i$ and $t_{m,k}^i$ are

$$c_{m,k}^i=(i+1)a_{m,k}^{i+1}\lambda_{m,k}^{i+1}-ka_{m,k}^i\lambda_{m,k}^i,$$
$$e_{m,k}^i=(i+1)d_{m,k}^{i+1}\lambda_{m,k}^{i+1}-kd_{m,k}^i\lambda_{m,k}^i,$$
$$s_{m,k}^i=(i+1)b_{m,k}^{i+1}\lambda_{m,k}^{i+1}-kb_{m,k}^i\lambda_{m,k}^i,$$
$$d_{m,k}^i=(i+1)(i+2)a_{m,k}^{i+2}\lambda_{m,k}^{i+2}-2k(i+1)a_{m,k}^{i+1}\lambda_{m,k}^{i+1}+k^2a_{m,k}^i\lambda_{m,k}^i,$$

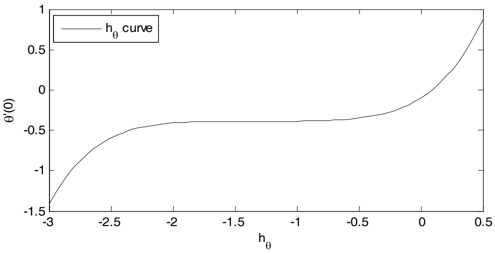


Fig. 1. The $h_\theta$ curve for 9th-order approximation of $\theta'(0)$ when $\lambda = 0.1,\ d = 0.5,\ M = 0.0,\ \Pr = 0.7,\ K_0 \to \infty$ .

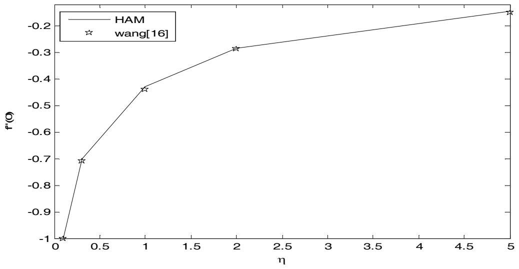


Fig. 2. Values of $f''(0)$ when $R = 0.0,\ M = 0.0,\ d = 0.0,\ n = 1.0$.

$$t^i_{m,k} = (i+1)(i+2)b^{i+2}_{m,k}\lambda^{i+2}_{m,k} - 2k(i+1)b^{i+1}_{m,k}\lambda^{i+1}_{m,k} + k^2 b^i_{m,k}\lambda^i_{m,k},$$

$$\lambda^i_{m,k} = \begin{cases} 0 & i = j = 0, k \geq 2 \ or \ i > 0, j = 0, k \geq 1, \\ 0 & j > i+1 \quad\quad or \quad\quad k > 2(i+1) - j, \\ 1 & \quad\quad\quad otherwise. \end{cases}$$

Using the above recurrence formulae, we can calculate all coefficients $a^i_{m,k}$ and $b^i_{m,k}$ by using only the first five given by the initial approximations:

$$a^0_{0,0} = R,\ a^1_{0,0} = d,\ a^1_{0,1} = \frac{1-d}{1+2\lambda},\ b^1_{0,0} = 1,\ b^1_{0,1} = 1 .$$

Therefore, the following explicit, totally analytic solutions of the present flow are

$$f(\eta) = \lim_{N\to\infty}\left(\sum_{m=0}^{N} a^0_{m,0} + \sum_{k=1}^{N+1}\sum_{m=k-1}^{2N}\sum_{i=0}^{2m+1-k} a^i_{m,k}\eta^i \exp(-k\eta)\right), \quad (30)$$

$$\theta(\eta) = \lim_{N\to\infty}\left(\sum_{m=0}^{N} b^0_{m,0} + \sum_{k=1}^{N+1}\sum_{m=k-1}^{2N}\sum_{i=0}^{2m+1-k} b^i_{m,k}\eta^i \exp(-k\eta)\right). \quad (31)$$

## 4. Results and discussion

The convergence and rate of approximation for the HAM solution strongly depend on the values of auxiliary parameters $h_f$ and $h_\theta$. To see the admissible values of $h_f$ and $h_\theta$, the h-curve is plotted in Fig. 1. Fig. 1 clearly elucidates that the range for the admissible values is $-2.5 \leq h_\theta \leq -0.5$ . It is founded that our analytic approximations for $h_f = -0.36$ agree well with the results of Wang [16], as shown in Fig. 2. Our computations show that the series of Eqs. (30) and (31) converge in the whole region of $\eta$ when $h_f = -0.56$ and $h_f = -1.5$ .

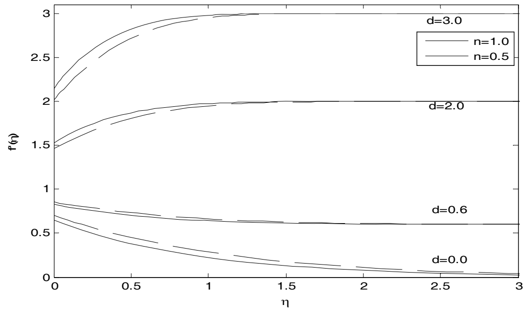


Fig. 3. Velocity profiles $f'(\eta)$ for different values of $d$ with $M = 0.5$, $R = 0.0$, $\lambda = 0.5$ .

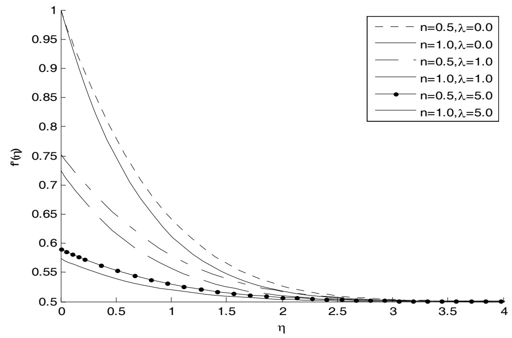


Fig. 4. Similarity velocity profiles $f'(\eta)$ for different values of $\lambda$ with $M = 0.5, R = 0.0,\ d = 0.5$.

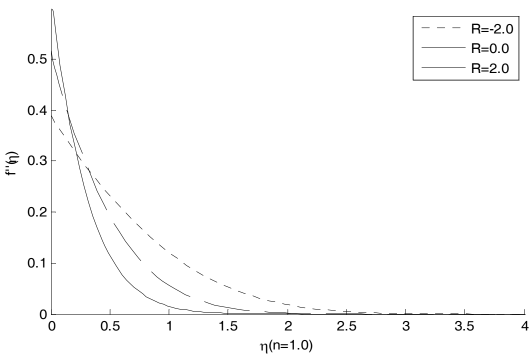


Fig. 5. Shear stress profiles $f''(\eta)$ for different values of $R$ with M = 1.0, $\lambda = 0.5$ n=1.0.

Figs. 3-5 present representative profiles for the tangential velocity profile $f'(\eta)$ and shear stress profile $f''(\eta)$ of plane and axisymmetric flows for various slip factors $\lambda$ and velocity radio parameters, respectively. Fig. 3 shows that the flow has a boundary layer when $d > 1$ . Furthermore, the thickness of the boundary layer decreases with increase in $d$ . On the other hand, an inverted boundary layer is formed when $d < 1$ . Slip velocity has the tendency to warm up and slow down the movement of the fluid. The effect of $\lambda$ on the tangential velocity depends on $d$. For $d > 1$, increasing $\lambda$ increases $f'(\eta)$ , while for $d < 1$ increasing $\lambda$ decreases $f'(\eta)$ . When $\lambda \to \infty$ (full slip), the solution is the potential flow $f(\eta) = d\eta + R$ . In Fig. 5, the influences of suction (R<0) and injection(R>0) are illustrated on shear stress profile $f''(\eta)$ .

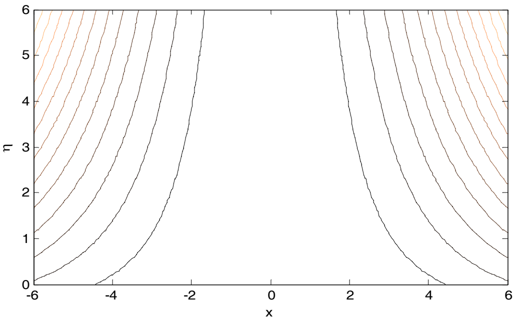


Fig. 6. The stream line profiles for axisymmetric flow with $\lambda = 5.0$, $d = 0.5$, $M = 0.5$, $R = 0.5$.

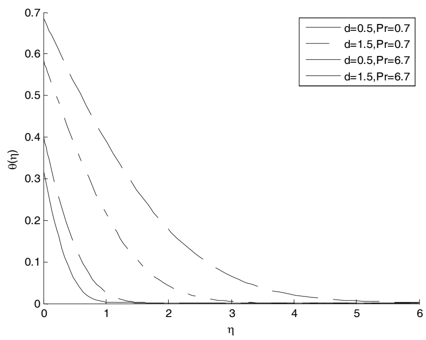


Fig. 7. Variation of $\theta(\eta)$ with Pr and $d$ at $R = 0.0$, $M = 0.0$, $K_0 = 0.8$, $\lambda = 1.0$, $\beta = 1.0$.

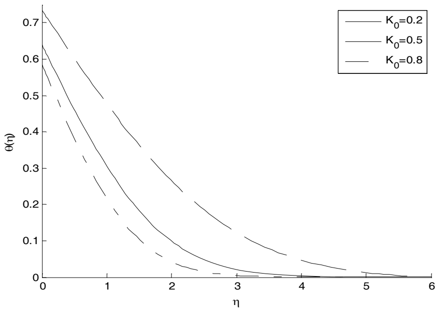


Fig. 8. Variation of $\theta(\eta)$ with $K_0$ at $R = 0.0$, $M = 0.0$, $\Pr = 0.7$, $\lambda = 1.0$, $\beta = 1.0$, $d = 1.5$.

It is seen that the effects of parameters R on the velocity $f'(\eta)$ and shear stress $f''(\eta)$ are similar to those of the slip parameter. The streamline pattern for axisymmetric flow for $\lambda = 5.0$, $d = 0.5$ $M = 0.5$, $R = 0.5$ is shown in Fig. 6.

Fig. 7 is made for the effects of Pr and d on the temperature field $\theta(\eta)$. Fig. 7 shows that temperature $\theta(\eta)$ decreases significantly with the increase in d. As anticipated, the thermal boundary layer thickness decreases with increasing Prandtl number. It is clear from this figure is that at a certain point, the temperature decreases with increase in Prandtl number Pr and the rate of heat transfer also decreases in this case. Fig. 8 shows the effects of radiation parameter $K_0$ on $\theta(\eta)$. It is obvious from Fig. 8 that the temperature $\theta(\eta)$ is a decreasing function of $K_0$.

Figs. 9 and 10 present the influence of the temperature jump parameter $\beta$ on $\theta(\eta)$ and $\theta'(\eta)$. Physically speaking, the presence of temperature jump has the tendency to decrease the fluid temperature while $\theta'(\eta)$ increases as $\beta$ becomes bigger.

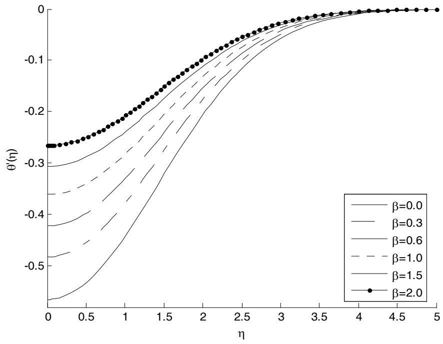


Fig. 9. Variation of $\theta'(\eta)$ with $\beta$ at $R = 0.0$, $M = 0.0$, $\Pr = 0.7$, $\lambda = 1.0$, $K_0 = 0.5$, $d = 1.5$.

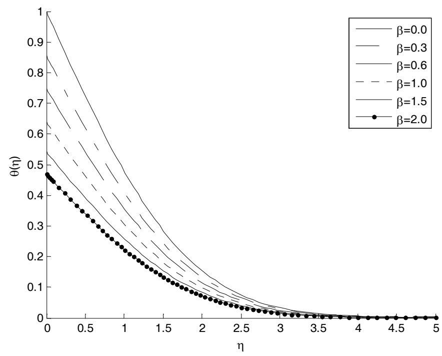


Fig. 10. Variation of $\theta(\eta)$ with $\beta$ at $R = 0.0$, $M = 0.0$, $\Pr = 0.7$, $\lambda = 1.0$, $K_0 = 0.5$, $d = 1.5$.

Finally, we compute the dimensionless shear stress $f''(0)$ at the wall and the heat-transfer coefficient $-\theta'(0)$ for the various parameters involved in the problem in Figs. 11-14 and Tables 1 and 2. Effect of slip parameter $\lambda$ on $f''(0)$ depends on $d$ as shown in Table 1. It can be seen that when $d < 1$, the wall shear $f''(0)$ increases with increase in $\lambda$. Yet, when $d > 1$, $f''(0)$ decreases with increase in $\lambda$. Application of a magnetic field has the tendency to warm up and slow down the movement of the fluid. Again, the plane flow values $|f''(0)|$ are higher than those for axisymmetric flow.

Figs. 11 and 12 present the influence of the temperature jump parameter, Prandtl number and the heat generation parameter on the temperature gradient at the wall. It is observed that $-\theta'(0)$ increases as Pr and $R$ increase and decreases as $\beta$ increases. Fig. 13 depicts the variations in $-\theta'(0)$ as a result of simultaneous increases in $M$ and $K_0$. The influence of $K_0$ and $M$ is to increase $-\theta'(0)$ with their increases. Fig. 14 shows that the magnitude of $-\theta'(0)$ increases with increases in $d$. Effect of slip parameter $\lambda$ on $-\theta'(0)$ is shown in Table 3. It can be seen that the heat transfer coefficient $-\theta'(0)$ decreases with increases in $\lambda$. The effects of all the parameters mentioned above on $-\theta'(0)$ were similar for axisymmetric flows and plane flows.

Table 1. Initial values $f''(0)$ ( $R = 0.0$, $d = 0.5$ ).

| $n$ | $n$=1.0 | | $n$=0.5 | |
|---|---|---|---|---|
| $\lambda$ | M=0.0 | M=0.5 | M=0.0 | M=0.5 |
| 0.0 | -0.66726 | -0.75401 | -0.53275 | -0.58661 |
| 0.1 | -0.58004 | -0.64689 | -0.47506 | -0.51855 |
| 0.5 | -0.38630 | -0.41795 | -0.33522 | -0.35861 |
| 1.0 | -0.27531 | -0.29221 | -0.24760 | -0.26107 |
| 2.0 | -0.17617 | -0.18348 | -0.16391 | -0.17203 |
| 5.0 | -0.08531 | -0.08712 | -0.08215 | -0.08388 |
| 10.0 | -0.04599 | -0.04653 | -0.04502 | -0.04556 |
| 30.0 | -0.01619 | -0.01626 | -0.01606 | -0.01614 |
| $\infty$ | 0.00000 | 0.00000 | 0.00000 | 0.00000 |

Table 2. Initial values $\theta'(0)$ ( $R = 0.0$, $d = 0.5$, $M = 0.0$, $\Pr = 0.7$, $K_0 = 0.8$ ).

| $n$ | $n$=1.0 | | $n$=0.5 | |
|---|---|---|---|---|
| $\lambda$ | $\beta$ =0.0 | $\beta$ =1.0 | $\beta$ =0.0 | $\beta$ =1.0 |
| 0.0 | -0.50159 | -0.33459 | -0.51104 | -0.33798 |
| 1.0 | -0.46011 | -0.31548 | -0.46916 | -0.31972 |
| 10.0 | -0.42759 | -0.30004 | -0.43256 | -0.30183 |
| 30.0 | -0.42507 | -0.29804 | -0.42624 | -0.29893 |

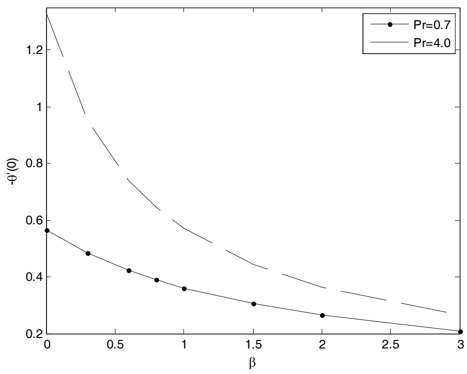


Fig. 11. Effects of $\beta$ on $-\theta'(0)$ at $R = 0.0$, $M = 0.0$, $\lambda = 1.0$, $K_0 = 0.5$, $d = 1.5$ .

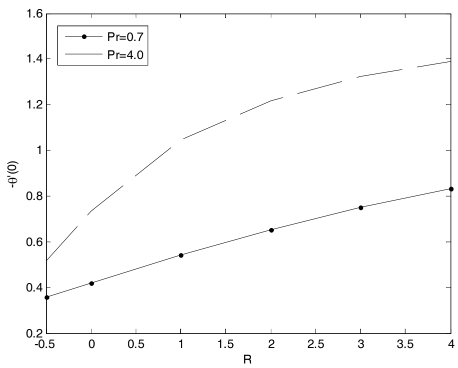


Fig. 12. Effects of $R$ on $-\theta'(0)$ at $M = 1.0$, $\lambda = 0.5$, $K_0 = 0.5$, $d = 1.5$, $\beta = 0.6$ .

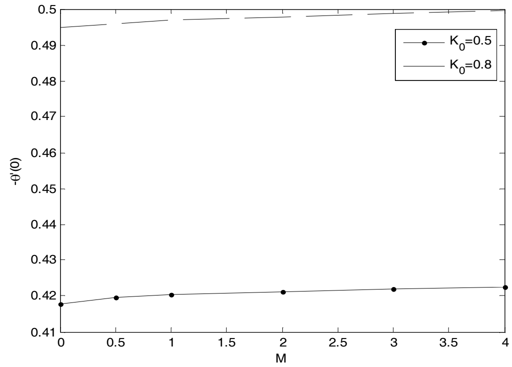


Fig. 13. Effects of $M$ on $-\theta'(0)$ at $R = 0.0$, $\lambda = 0.5$, $\Pr = 0.7$, $d = 1.5$, $\beta = 0.6$ .

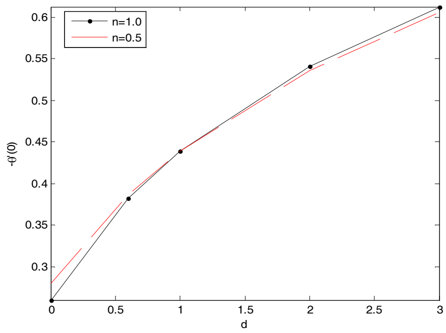


Fig. 14. Effects of $d$ on $-\theta'(0)$ at $R = 0.0$, $\lambda = 0.5$, $\Pr = 0.7$, $\beta = 0.6$, $M = 0.5$, $K_0 = 0.8$ .

## 5. Conclusions

The present paper theoretically studies the plane and axisymmetric stagnation flows and heat transfer towards a stretching sheet with velocity slip and temperature jump. The governing equations are transformed to ordinary differential equations by exploiting the similarity procedure. The resulting equation system is then solved analytically by using HAM. The velocity and temperature field are obtained in the form of series. The effects of the different emerging parameters are shown through some graphs. The values of the skin friction coefficient and the surface heat transfer coefficient are also given. From this analysis, we have made the following observations:

(1) The dimensionless velocity $f'(\eta)$ decreases with increases in $R, \lambda$ and $M, n$ when $d > 1$. However, the opposite behavior has been found for $d < 1$.

(2) The plane and axisymmetric stagnation flows depend heavily on the velocity slip factor. Also, increasing values of $\lambda$ decreases the variation of $|f''(0)|$ and makes the surface shear stress $|f''(0)|$ close to 0 with $\lambda \to \infty$ .

(3) Shear stress at the surface $f''(0)$ increases with increase in $d$ as long as $d > 1$, but it decreases with increasing $d$ when $d < 1$.

(4) The dimensionless temperature field $\theta(\eta)$ decreases when $\Pr, d$ and $K_0, \beta$ increase for the plane and axisymmetric flow. However, the variation $\theta'(\eta)$ has the opposite

behavior for the temperature jump parameter $\beta$ .

(5) The magnitudes of the surface heat transfer $-\theta'(0)$ increase with increasing of parameter $\Pr, d$ and $R, K_0$ . However, the variation $-\theta'(0)$ has the opposite behavior for the temperature jump parameter $\beta$ .

## Acknowledgment

The work is supported by the National Natural Science Foundations of China (No. 50936003), the open Project of State Key Laboratory for Advanced Metals and Materials (2009Z-02) and Research Foundation of Engineering Research Institute, University of Science and Technology Beijing.

## References

[1] K. Hiemenz, Die Grenzschicht an einem in den gleichformigen Fluessigkeitsstrom eingetauchten geraden Kreiszylinder, *Dinglers Polytechnisches J.,* 326 (1911) 321-410.

[2] T. Chiam, Stagnation-point flow towards a stretching plate, *J. Phys. Soc. Jpn.,* 63 (6) (1994) 2443-2444.

[3] T. R. Mahapatra and A. S.Gupta, Heat transfer in stagnation-point flow towards a stretching sheet, *Heat Mass. Tran,* 38(6) (2002) 517-521.

[4] A. Ishak, R. Nazar and I. Pop, Dual solutions in mixed convection flow near a stagnation point on a vertical surface in a porous medium, *Int. J. Heat Mass Tran.,* 51 (5-6) (2008) 1150-1155.

[5] A. Raptis, Flow of a micropolar fluid past a continuously moving plate by the presence of radiation, *Int. J. Heat Mass Transfer,* 41 (18) (1998) 2865-2866.

[6] H. A. M. El-Arabawy, Effect of suction/injection on the flow of a micropolar fluid past a continuously moving plate in the presence of radiation, *Int. J. Heat Mass Transfer,* 46 (8) (2003) 1471-1477.

[7] S. K. Khan, Heat transfer in a viscoelastic fluid flow over a stretching surface with heat source/sink, suction/blowing and radiation, *Int. J. Heat Mass Transfer*, 49 (3-4) (2006) 628-639.

[8] A. Yoshimura and R. K. Prudhomme, Wall slip correc-tions for Couette and parallel disc viscometers, *J. Rheol*, 32 (1) (1988) 53-67.

[9] M. Mooney, Explicit formulas for slip and fluidity. *J. Rheology*, 2 (2) (1931) 210-222.

[10] I. J. Rao and K. R. Rajagopal, The effect of the slip condition on the flow of fluids in a channel, *Acta Mech.,* 135 (3) (1999) 113-126.

[11] A. R. A. Khaled and K. Vafai, The effect of slip condition on Stokes and Couette flows due to an oscillating wall: exact solutions, *Int. J. Non-Linear Mech,* 39 (5) (2004) 795-804.

[12] T. Hayat, K. Masood and M. Ayub, The effect of the slip condition on flows of an Oldroyd 6-constant fluid, *J. Comput. Appl. Math,* 202 (2) (2007) 402-413.

[13] R. C. Chaudnary, A. K. Jiha and F. Hang, Effects of chemical reaction on MHD micropolar fluid flow past a vertical plate in slip-flow regime, *Appl. Math. Mech.,* 29 (9) (2008) 1179-1194.

[14] H. I. Andersson and M. Rousselet, Slip flow over a lubricated rotating disk, *Int. J. Heat.Fluid Flow,* 27 (2) (2006) 329-335.

[15] F. Labropulu and D. Li, Stagnation-point flow of a second-grade fluid with slip, *Int. J. Non-Linear Mech,* 43 (9) (2008) 941-947.

[16] C. Y. Wang, Flow due to a stretching boundary with partial slip—an exact solution of the Navier–Stokes equations, *Chem. Eng. Sci,* 57 (17) (2002) 3745-3747.

[17] C. Y. Wang, Stagnation slip flow and heat transfer on a moving plate, *Chem. Eng. Sci.,* 61 (23) (2006) 7668-7672.

[18] S. J. Liao, Beyond perturbation: introduction to homo-topy analysis method, Boca Raton, Chapman (2003).

[19] J. Zhu, L. C. Zheng and X. X. Zhang, Analytic solution of stagnation-point flow and heat transfer over a stretching sheet based on homotopy analysis, *Appl. Math. Mech.,* 30 (4) (2009) 463-474.

[20] T. Hayat Z. Abbas and M. Sajid, Series solution for the upper-convected Maxwell fluid over a porous streching plate, *Phys. Lett. A*, 358 (5-6) (2006) 396-403.

[21] C. Wang and I. Pop, Analysis of the flow of a power-law fluid film on an unsteady stretching surface by means of homotopy analysis method, *Journal of Non-Newtonian Fluid Mechanics*, 138 (2-3) (2006) 161-172.

[22] M. M. Ali, T. S. Chen and B. F. Armaly, Natural convection-radiation interaction in boundary layer flow over horizontal surfaces, *AIAA. J.,* 22 (12) (1984) 1797-1803.

**Jing Zhu**, Ph.D, Department of Mathematics and Mechanics, University of Science and Technology Beijing, P.R. China. Her research fields are Thermal Engineering, Fluid Mechanics, Applied mathematics and Nonlinear Mechanics. In the past 5 years, she has taken part in 3 kinds of research projects and has published more than 8 papers on domestic and overseas science journals, 6 of which were embodied by SCI and EI.